

Application to radiative acoustics of Whitham's method for the analysis of non-equilibrium wave phenomena

By A. C. COGLEY † AND W. G. VINCENTI

Department of Aeronautics and Astronautics, Stanford University

(Received 19 December 1968 and in revised form 26 June 1969)

An approximate method due originally to Whitham is applied to the study of acoustic waves propagating in a non-grey radiating and absorbing gas, assumed in local molecular equilibrium. The method, which has general applicability in the study of non-equilibrium wave phenomena, replaces the exact governing equation by a set of lower-order equations that can be solved analytically in many cases. The use of the method is demonstrated by reconsidering the one-dimensional problems of (i) harmonic waves driven by a harmonic variation in either position or temperature of a planar wall and (ii) the discrete wave produced by the impulsive motion of a constant-temperature wall. The method greatly simplifies the mathematics for these problems, and comparison of the results with those of earlier investigators shows the approximate method to be accurate. Moreover, the method allows us to obtain a more systematic and complete analytical solution of the second problem than has been obtained by more conventional methods.

1. Introduction

In their mathematical aspects, this and the companion paper that follows are an extension of a method due originally to Whitham (1959). This method is suitable for the approximate solution of problems of wave propagation when more than one propagation speed appears in the governing differential equations, as is the case when non-equilibrium processes occur within the fluid. Although Whitham concerned himself with application to magnetohydrodynamics, his ideas apply generally to other dissipative processes in both linear and non-linear situations. Here we shall restrict ourselves to linear problems only. As shown by Whitham, however, linear solutions are an important first step in the understanding of the corresponding non-linear phenomena.

In a physical sense, the present work is a continuation of recent studies of the interaction of radiative transfer and fluid flow in the acoustic approximation. It follows in particular in the spirit of papers by Vincenti & Baldwin (1962), Baldwin (1962), Lick (1964) and Moore (1966). (For reference to earlier work see the first of these; for pedagogical treatments see Vincenti & Kruger 1965, or Lick 1967.) As in those papers, we deal with one-dimensional acoustic waves in

† Present address: Department of Energy Engineering, University of Illinois, Chicago.

the semi-infinite expanse of gas to one side of an infinite planar black wall. The gas is assumed to be thermally perfect and in local molecular equilibrium. In contrast to the previous work, however, it is not taken to be grey (i.e. absorption coefficient independent of radiative frequency). Instead, non-grey effects are included on the basis of the generalized substitute-kernel approximation developed by Gilles, Cogley & Vincenti (1969).

In the present paper we develop the formalism for application of Whitham's method in radiative acoustics and use it to solve problems that have already yielded to other methods. These are the harmonic waves due to sinusoidal motion and temperature variation of the wall and the discrete wave due to impulsive motion of the wall at constant temperature. Comparison with the previous results then establishes the interpretation, accuracy and usefulness of the approximate method. In Cogley (1969) the method will be employed to solve the more difficult problem of the discrete wave caused by a step change in temperature of a motionless wall. This has previously eluded solution by other methods except in a very restricted way. The two papers together illustrate the power of Whitham's approach, not only for a qualitative understanding of wave phenomena, but for the detailed solution of specific problems.

Whitham's method is based on the physical idea that, in one-dimensional wave motion, the wave-form appears almost invariant when followed at its own speed of propagation. Put in mathematical terms, this idea enables one to replace the exact governing equation by a set of approximate, lower-order equations, each of which is valid in a specified region of the time-like variable. A different lower-order equation is obtained for each propagation speed appearing in the exact equation. The boundary conditions for the exact problem can be used with these lower-order equations, if one is careful to include all the boundary layers and purely diffusive waves present. The resulting solutions of the lower-order equations, obtainable in closed form in many cases, then represent portions of the total solution. The relatively simple form of the lower-order equations also tells one explicitly, without formal solution of the problem, what type of response to expect. The method also has the advantage of dividing the problem into physically meaningful parts, so that one is able to see how and why the resulting wave forms develop. These matters are elaborated on in §2 for Whitham's simple model equation and in §3 for the acoustic equation of radiative gas dynamics. In the latter case we see in particular how the exact fifth-order equation containing four propagation speeds is replaced by four approximate lower-order equations.

To test the accuracy and usefulness of the method (and, as it turns out, to obtain insight into the significance of the lower-order equations), the problem of harmonic waves is reconsidered in §4. Vincenti & Baldwin (1962), in their work based on the exact equation, found the solution to be the sum of two types of waves, which they referred to as 'modified-classical' and 'radiation-induced'. The approximate method essentially reproduces these results, with the modified-classical wave being governed by two of the four lower-order equations and the radiation-induced wave by the other two. One equation from each pair is valid in specified frequency ranges, and these frequency ranges depend in turn on the

dimensionless parameter that specifies the level of radiative transfer. The accuracy of the results, as revealed by comparison with a numerical solution of the exact equation, is excellent over wide ranges of frequency for all levels of radiative transfer. Exceptions occur in small regions of frequency, where the solution changes from one lower-order equation to the other, but even there the results are not seriously off.

The solution for the discrete wave due to impulsive motion of the constant-temperature wall is obtained in §5 and §6. For this purpose, each of the approximate lower-order equations is solved formally by means of the Laplace transform, which effectively superposes the corresponding harmonic solutions. Each transformed solution applies in certain ranges of the transformation variable and hence, by the Abelian theorems, in certain regions of time when the solution is inverted. The time regions of validity for this unsteady problem are determined by the frequency ranges of validity of the corresponding harmonic solutions and thus depend on the level of radiative transfer. As with the purely harmonic waves, the complete solution in a given time region is the sum of two of the four approximate solutions, one from the pair of lower-order equations that governs the modified-classical waves and one from the pair that governs the radiation-induced waves. These matters are set down in detail in §5, together with the boundary conditions for step changes in both velocity and temperature of the wall.

The application to the impulsively moving wall is given in §6. In obtaining the inversions of the transformed solution, advantage is taken of expansions consistent with the various regions of validity. This allows solutions to be obtained in closed form throughout. The final results for the wave-front, which is formed by the modified-classical contribution, are found to agree closely with those from existing studies. The main item of interest, however, is the complete treatment of the diffusing thermal layer that forms next to the constant-temperature wall even under conditions of weak radiation. This boundary layer comes from the radiation-induced contribution and is physically necessary under all conditions to bring the final temperature of the compressed gas adjacent to the wall back to that of the wall itself. To the order of the solution, the layer is found to affect only the temperature and density of the gas. The relation of these results to earlier studies is explained after the results are presented.

2. Introduction to Whitham's method

Whitham gives a detailed discussion of his approximate method for a simple model equation. Certain of his results are summarized and generalized here to give the reader an introduction to the basic idea. Whitham's method applies directly to the simplification of the governing differential equation and is not to be confused with other approximations that will be introduced later. These will serve only to simplify the formal solution of some particular approximate equation.

Expressed mathematically, the basic idea of Whitham's method is that a planar wave form appears almost steady or invariant when described in terms

of slant co-ordinates based on the wave's particular speed of propagation. In classical (i.e. non-dissipative) acoustic theory this condition is satisfied exactly in the slant co-ordinate based on the one unique speed of propagation. In non-equilibrium acoustic theory, more than one propagation speed may appear, and we must consider slant co-ordinates based on each speed separately to obtain an overall view of the wave phenomena. The mathematical consequence of the basic idea is that we can replace the exact governing differential equation by a set of lower-order equations, one for each propagation speed. Each of these is part of a valid approximation to the exact equation in a specified region of the independent time-like variable. Often, in particular in radiative acoustics, so-called degenerate speeds with values of zero and infinity appear. These degenerate speeds may represent diffusive mechanisms that give rise to either boundary layers or purely diffusive waves.† Which of these is present depends on the specific equation under study and on the type of boundary condition that drives the wave. When the equations that govern the purely diffusive waves and boundary layers are included in the set of equivalent lower-order equations, the exact boundary conditions can be used with this set.

Whitham's method is of a heuristic nature and does not proceed from a mathematically rigorous argument. Its accuracy is therefore not given as an integral part of the method. The same lower-order equations, however, can be generated by formal asymptotic co-ordinate and parameter expansions, and these equivalent expansions provide insight into the accuracy of the method and show how and why it works. This approach has been carried through by Cogley (1968) for acoustic propagation with chemical non-equilibrium. The equivalent asymptotic expansions are not always easily obtained for more complex problems, and the details of the procedure have not been carried out for the equation of radiative acoustics. Instead we follow a more pragmatic course and gain an understanding of the method by using it to solve certain example problems.

Most of the problems with which we deal can be called signalling problems. These are the special form of general, one-dimensional, wave-propagation problems in which homogeneous initial conditions are assumed, the domain is the semi-infinite space, and only waves propagating to the right from a disturbance at the origin are considered. The disturbance is taken as a step input in some dependent variable, unless stated otherwise.

The ideas of the preceding paragraphs can be made explicit by discussing Whitham's simple, example equation

$$\left(\frac{\partial}{\partial t} + c_1 \frac{\partial}{\partial x}\right) \left(\frac{\partial}{\partial t} + c_2 \frac{\partial}{\partial x}\right) \phi' + K \left(\frac{\partial}{\partial t} + a \frac{\partial}{\partial x}\right) \phi' = 0, \quad (1)$$

where ϕ' is any perturbation quantity, K (assumed positive) is a given parameter with dimensions of (time)⁻¹, t is the time, and x the space co-ordinate. The real, distinct constants c_1 , c_2 and a are propagation speeds. Approximate equations governing the various wave motions implicit in (1) are found by transforming

† The expression 'may represent' is used here because the appearance of a zero propagation speed does not always represent a diffusive mechanism (cf. Cogley 1968, ch. 3).

to slant co-ordinates for a particular propagation speed and dropping certain higher-order terms. The same end can be accomplished in one step in Cartesian co-ordinates by stating that the derivatives $\partial/\partial t$ and $-c\partial/\partial x$ of any dependent variable are approximately equal for a wave travelling with speed c .

When the speed c_1 is followed, (1) may be approximated on the basis of the foregoing procedure by

$$\left(\frac{\partial}{\partial t} + c_1 \frac{\partial}{\partial x}\right) \phi' + K \left(\frac{c_1 - a}{c_1 - c_2}\right) \phi' = 0, \quad (2)$$

where $(c_1 - a)/(c_1 - c_2)$ must be positive for a stable (i.e. damped) solution to exist (cf. Whitham 1959). To obtain this equation, an integration has been performed and the function of integration set equal to zero, as is appropriate when homogeneous initial conditions are assumed. It is to be understood that this procedure will always be carried out where applicable. Equation (2) governs the wave motion only at some small time, since its solution, with a step input in ϕ' , is an exponentially damped step wave that becomes practically non-existent at larger times. The precise condition is that (2) is a valid approximation of (1) for $Kt \ll 1$.

We follow the wave speed a in a similar manner by setting $\partial/\partial t \cong -a\partial/\partial x$. Equation (1) may then be approximated by

$$\frac{(c_1 - a)(a - c_2)}{K} \frac{\partial^2 \phi'}{\partial x^2} - \left(\frac{\partial}{\partial t} + a \frac{\partial}{\partial x}\right) \phi' = 0. \dagger \quad (3)$$

This equation governs the wave motion for large time, since its solution is a wave that does not decay; it does diffuse, however, with a diffusion coefficient proportional to $1/K$. More precisely, (3) is a valid approximation of (1) for $Kt \gg 1$.

If $c_2 < 0$, there is no need to follow this speed, since we are interested only in waves travelling to the right. Equation (1) then requires one boundary condition at $x = 0$; (2) and (3) also require one boundary condition. Thus, the boundary condition for the exact equation (1) can also be used with these simplified equations. The fact that the simplified equations require fewer initial conditions is of no concern, since we assume the gas to be quiescent for $t \leq 0$.

When $c_2 > 0$, this speed must also be followed. Setting $\partial/\partial t \cong -c_2\partial/\partial x$ leads to the lower-order equation

$$\left(\frac{\partial}{\partial t} + c_2 \frac{\partial}{\partial x}\right) \phi' + K \left(\frac{a - c_2}{c_1 - c_2}\right) \phi' = 0, \quad (4)$$

whose solution for a step input in ϕ' is an exponentially decaying step wave when $(a - c_2)/(c_1 - c_2)$ is positive. Equation (1) plus two boundary conditions form a well-posed problem, since we now have two characteristics pointing into the region of interest. The simplified equations (2)–(4), on the other hand, each form a well-posed problem with only one boundary condition. For $Kt \ll 1$, (2) and (4) are simultaneously valid, and together they absorb the two exact

† This approximate equation is not of lower order than the exact equation (1). This is due to the oversimplified example. All the problems of radiative acoustics in this work will have approximate equations of lower order than the exact equation.

boundary conditions. For $Kt \gg 1$, however, (3) alone is valid, and this equation can absorb only one condition. The inconsistency can be resolved by assuming that a boundary layer exists near $x = 0$. An equation governing this boundary layer is obtained by assuming the layer to be thin, so that the x derivatives are much larger than the t derivatives. This boundary-layer argument is analogous to having a zero propagation speed appear in the exact solution. In radiative acoustics we will follow a zero speed by assuming $\partial/\partial t = -\partial/\partial x$, which is essentially the same as saying that $\partial/\partial t \ll \partial/\partial x$. Equation (1) is approximated accordingly by

$$c_1 c_2 \frac{\partial \phi'}{\partial x} + Ka\phi' = 0. \quad (5)$$

This equation is used in conjunction with (3) to absorb the two given boundary conditions at the larger times in the approximate solution.

Whitham also developed criteria for stable solutions to exist for general signalling equations similar to (1). Here stability means that a solution of the given equation does not grow without bound. It turns out that the question of stability is unimportant for our problems, i.e. the solutions that we seek are all inherently stable. The reader is therefore referred to Cogley (1968) for a discussion of stability for the radiative acoustic equation.

3. Basis for application to radiative acoustics

The governing equation for acoustic propagation in a non-grey radiating and absorbing gas has been derived by Gilles, Cogley & Vincenti (1969). As usual, radiative scattering, pressure, and energy density are taken to be negligible. In general, as in the reference, the derivation can be carried out for an imperfect gas; purely for convenience we here assume the gas to be thermally, but not necessarily calorically, perfect. Radiative effects are taken into account on the hypothesis of local molecular equilibrium, and a non-grey exponential (substitute-kernel) approximation is employed. This approximation introduces two functions $m_0(p_0, T_0)$ and $n_0(p_0, T_0)$, where p_0 and T_0 are the undisturbed pressure and temperature respectively. † The function n_0 is an effective frequency-averaged absorption coefficient, and m_0 is associated with the rate of spontaneous emission, as will be pointed out later. Specific functional forms for these quantities are developed in the reference. Here, however, we leave the formulation general and carry out all work in normalized variables and parameters.

The normalized equation governing radiative acoustics can be written in terms of a dimensionless potential function ϕ defined by the relations

$$\phi_\xi = u \equiv u'/a_{S_0}, \quad \phi_\tau = -p/\gamma_0 \equiv -(1/\gamma_0)p'/p_0.$$

† If the gas is strongly non-grey in the sense that the absorption coefficient is a widely varying function of frequency, an improved, many-parameter fit for the exact radiative transmission functions can be obtained by using a sum of exponentials in place of the single exponential used here. For each additional exponential the resulting partial differential equation increases by two orders in the spatial variable (cf. Gilles, Cogley & Vincenti 1969). Each added exponential thus adds another radiation-induced wave to the one appearing here. The generality of Whitham's method should allow one to handle these additional waves.

The normalized independent variables are $\xi \equiv n_0 x$ and $\tau \equiv n_0 a_{S_0} t$; as subscripts they denote partial differentiation. Normalized perturbations in velocity and pressure are symbolized by u and p . The convention of using unadorned symbols for normalized perturbation variables will be used throughout. Primed symbols will denote the corresponding dimensional perturbations. Symbols subscripted by 0 are dimensional quantities in the undisturbed reference state, which is one of complete equilibrium. The isentropic sound speed a_{S_0} is given for the thermally perfect but calorically imperfect gas by

$$a_{S_0} = (\gamma_0 p_0 / \rho_0)^{\frac{1}{2}},$$

where ρ_0 is the undisturbed density and γ_0 is the ratio of specific heats. We can also regard γ_0 as a measure of the ratio of the isentropic sound speed to the isothermal sound speed $a_{T_0} = (p_0 / \rho_0)^{\frac{1}{2}}$, i.e.

$$\sqrt{\gamma_0} = a_{S_0} / a_{T_0}.$$

With the foregoing nomenclature, the equation of radiative acoustics can be written as

$$(\phi_{\tau\tau} - \phi_{\xi\xi})_{\xi\xi\tau} + \frac{16\gamma_0}{Bo_N} \left(\phi_{\tau\tau} - \frac{1}{\gamma_0} \phi_{\xi\xi} \right)_{\xi\xi} - (\phi_{\tau\tau} - \phi_{\xi\xi})_{\tau} = 0, \tag{6}$$

where the effective non-grey Boltzmann number, a measure of the ratio of the mechanical to the radiative energy flux, is defined by

$$Bo_N \equiv \frac{n_0 \gamma_0 \rho_0 a_{S_0} R}{m_0 (\gamma_0 - 1) (\pi/4) \hat{B}_{T_0}} = \frac{n_0}{m_0} \hat{B}_0.$$

The quantity \hat{B}_0 is the non-grey Boltzmann number introduced by Gilles, Cogley & Vincenti, and R is the ordinary gas constant. The symbol \hat{B}_{T_0} is defined as

$$\hat{B}_{T_0} \equiv \int_{\alpha_{\nu_0} \neq 0} \left. \frac{dB_{\nu}}{dT} \right|_0 d\nu,$$

where B_{ν} and α_{ν} are the Planck function and the volumetric absorption coefficient, both functions of the spectral frequency ν . The integration is over all frequencies for which α_{ν_0} is non-zero. The precise meaning of m_0 is that the combination $4m_0 \hat{B}_{T_0} T'$ gives the perturbation in the rate of spontaneous radiative emission per unit volume for a non-grey gas. With ϕ known, the normalized perturbation density $\rho \equiv \rho' / \rho_0$, temperature $T \equiv T' / T_0$, enthalpy $h \equiv h' (\gamma_0 - 1) / \gamma_0 R T_0$, and effective radiative heat flux $\hat{q}^R \equiv \hat{q}^R (\gamma_0 - 1) / \gamma_0 R T_0 \rho_0 a_{S_0}$ can be found from the linearized continuity equation

$$\rho_{\tau} + u_{\xi} = 0,$$

the linearized equations of state

$$T = p - \rho = h,$$

and the following relation for the radiative heat flux at frequencies where $\alpha_{\nu_0} \neq 0$ (cf. Vincenti & Kruger 1965):

$$\hat{q}_{\xi}^R = \phi_{\tau\tau} - \phi_{\xi\xi}.$$

To apply Whitham's ideas we first write (6) in the signalling form

$$\begin{aligned} & \left(\frac{1}{\infty} \frac{\partial}{\partial \tau} + \frac{\partial}{\partial \xi}\right) \left(\frac{1}{\infty} \frac{\partial}{\partial \tau} - \frac{\partial}{\partial \xi}\right) \left(\frac{\partial}{\partial \tau} + 0 \frac{\partial}{\partial \xi}\right) \left(\frac{\partial}{\partial \tau} + \frac{\partial}{\partial \xi}\right) \left(\frac{\partial}{\partial \tau} - \frac{\partial}{\partial \xi}\right) \phi \\ & + \frac{16\gamma_0}{Bo_N} \left(\frac{1}{\infty} \frac{\partial}{\partial \tau} + \frac{\partial}{\partial \xi}\right) \left(\frac{1}{\infty} \frac{\partial}{\partial \tau} - \frac{\partial}{\partial \xi}\right) \left(\frac{\partial}{\partial \tau} + \frac{1}{\sqrt{\gamma_0}} \frac{\partial}{\partial \xi}\right) \left(\frac{\partial}{\partial \tau} - \frac{1}{\sqrt{\gamma_0}} \frac{\partial}{\partial \xi}\right) \phi \\ & + \left(\frac{\partial}{\partial \tau} + 0 \frac{\partial}{\partial \xi}\right) \left(\frac{\partial}{\partial \tau} + \frac{\partial}{\partial \xi}\right) \left(\frac{\partial}{\partial \tau} - \frac{\partial}{\partial \xi}\right) \phi = 0. \end{aligned} \tag{7}$$

Four distinct propagation speeds are now evident in this equation. These speeds appear as multiplying factors with the operator $\partial/\partial\xi$ or, equivalently, their inverse multiplies the operator $\partial/\partial\tau$. By virtue of the normalization, the isentropic speed of sound is counted as unity and the isothermal speed of sound as $1/\sqrt{\gamma_0}$. The zero propagation speed appears as a zero multiplying the operator $\partial/\partial\xi$. The infinite speed, because of its singular nature, appears as $1/\infty$ multiplying $\partial/\partial\tau$. This is merely a convention used to write the radiative acoustic equation in signalling form. Physically, one may think of $1/\infty$ as being the limit of unity over the speed of light as this speed goes to infinity, since an infinite photon speed was assumed in the derivation of (6). To study the wave phenomena implicit in (7), we shall follow the four distinct propagation speeds at which information can be transmitted through the medium.

Employing the procedures of §2, we follow the isentropic speed in the positive- ξ direction by setting $\partial/\partial\tau \cong -\partial/\partial\xi$. We thus approximate equation (7) by

$$(\phi_\tau + \phi_\xi)_{\tau\tau} + \frac{8(\gamma_0 - 1)}{Bo_N} \phi_{\tau\tau} - (\phi_\tau + \phi_\xi) = 0. \tag{8}$$

This equation is essentially hyperbolic in character and contains the isentropic signalling operator in the first and last terms.

Information transmitted with the isothermal speed of sound is studied by taking $\partial/\partial\tau \cong -(1/\sqrt{\gamma_0})\partial/\partial\xi$. This allows us to replace (7) by

$$\phi_{\tau\tau} - \frac{32\gamma_0}{Bo_N(\gamma_0 - 1)} \left(\phi_\tau + \frac{1}{\sqrt{\gamma_0}} \phi_\xi\right) - \frac{1}{\gamma_0} \phi = 0. \tag{9}$$

This equation is also essentially hyperbolic with an isothermal signalling operator in the middle term.

The infinite-speed lower-order equation is similarly obtained by letting $\partial/\partial\tau \cong -\infty\partial/\partial\xi$. This results in approximating (7) by

$$\phi_{\xi\xi\tau} + \frac{16\gamma_0}{Bo_N} \phi_{\xi\xi} - \phi_\tau = 0. \tag{10}$$

This equation is essentially parabolic in character by virtue of the form of the last two terms. The infinite speed is present in the theory because radiative information is transmitted basically with the speed of light, which is here assumed infinite.

Since the radiative information in the diffusion limit effectively penetrates the medium only to a characteristic depth proportional to $\sqrt{\tau}$, this information appears to travel much slower than that carried by isentropic or isothermal waves, which penetrate to a depth proportional to τ . A zero speed is thus to be expected in the theory. Following this speed by taking $\partial/\partial\tau \cong -0\partial/\partial\xi$, we obtain the zero-speed lower-order equation

$$\phi_{\xi\xi\tau} + \frac{16}{Bo_N} \phi_{\xi\xi} - \phi_\tau = 0. \tag{11}$$

This equation is also essentially parabolic.

The appearance of the parabolic-like equations (10) and (11) is not surprising, since a hyperbolic equation reduces to the normal form of a parabolic equation (cf. Courant & Hilbert 1952, p. 157) when the propagation speed goes to either zero or infinity. That is, a zero or infinite propagation speed represents a diffusive phenomenon. Equations (10) and (11) differ only by the factor γ_0 in the second term of (10). The physical reason for this near identity, however, is not clear.

The equations (8)–(11) comprise the set of approximate lower-order equations that replaces the single exact equation (7). A certain amount of information concerning these lower-order equations and their solutions can be obtained from the equations themselves by mathematical arguments (cf. Whitham 1959 and Cogley 1968). A complete understanding of these still fairly complex equations can best be obtained, however, by comparing their solutions for certain example problems with those obtained from (7) by means of more conventional techniques.

The four boundary conditions needed to form the general well-posed problem for the exact equation (7) can be written as follows (cf. Gilles *et al.* 1969):

For $\xi = 0$:

$$\phi_\xi|_{\xi=0} = u_w(\tau), \tag{12}$$

$$\begin{aligned} & \frac{Bo_N}{16} [(\phi_{\tau\tau} - \phi_{\xi\xi})_{\xi\tau} - (\phi_{\tau\tau} - \phi_{\xi\xi})_\tau]_{\xi=0} \\ & + \gamma_0 \left[\left(\phi_{\tau\tau} - \frac{1}{\gamma_0} \phi_{\xi\xi} \right)_\xi - \left(\phi_{\tau\tau} - \frac{1}{\gamma_0} \phi_{\xi\xi} \right) \right]_{\xi=0} = \frac{dT_w(\tau)}{d\tau}. \end{aligned} \tag{13}$$

For $\xi \rightarrow \infty$:

$$\phi_\xi|_{\xi \rightarrow \infty} \rightarrow 0, \quad \phi_\tau|_{\xi \rightarrow \infty} \rightarrow 0. \tag{14}$$

In conditions (12) and (13) the subscript w denotes the perturbation velocity and temperature of the wall, which is located initially at $\xi = 0$. These conditions are applied at the origin, as is consistent with linearized theory. As stated earlier, the gas is initially quiescent.

The exact equation (7) needs the two near boundary conditions (12) and (13) to drive the two waves that propagate in the positive- ξ direction. The lower-order equations, however, need only one near boundary condition each to drive one outgoing wave. The seeming dilemma as to which boundary condition to use with a given lower-order equation is resolved by the fact that two of the lower-order equations are needed to replace the exact equation to obtain a solution at any given time. The exact boundary conditions (12) and (13) are thus used with

the lower-order equations, *taken two at a time*. The two equations together then form a well-posed problem with the two near boundary conditions. The question as to which two lower-order equations to use in a given time-like region is answered in the work that follows.

4. Harmonic waves

In this article we study the harmonic solutions of the lower-order equations. Harmonic solutions of the exact equation (7) have previously been studied analytically by Vincenti & Baldwin (1962), using the exponential approximation and the assumption of a grey gas. Long & Vincenti (1967) programmed the grey-gas solution on a computer in connexion with their study of radiatively driven harmonic waves in a closed tube, and their numerical program is easily modified to accommodate the present non-grey formulation. The latter 'exact' results are used here as a measure of the accuracy of the approximate solution.

To begin, we ignore the boundary conditions and examine the damping and wave speed of the harmonic solutions. As usual, it is convenient to introduce a new dimensionless distance and time defined by $\bar{x} \equiv \omega x/a_{S_0}$ and $\bar{t} = \omega t$, where ω is the radian frequency of the harmonic wave. These new variables are related to those introduced in §3 by

$$\xi = Bu_N \bar{x}, \quad \tau = Bu_N \bar{t}, \quad (15)$$

where the non-grey Bouguer number is defined by

$$Bu_N \equiv \frac{n_0 a_{S_0}}{\omega}.$$

A new potential function ψ is also introduced such that

$$\psi(\bar{x}, \bar{t}) \equiv \frac{\gamma_0}{Bu_N} \phi(\xi, \tau). \quad (16)$$

The dimensionless perturbation velocity and pressure are now given accordingly by

$$u = \frac{1}{\gamma_0} \frac{\partial \psi}{\partial \bar{x}}, \quad p = -\frac{\partial \psi}{\partial \bar{t}}.$$

The quantity γ_0 is included in the definition (16) to make the present normalization compatible with the previous work of Vincenti & Baldwin (1962) and Cheng (1966). For all four lower-order equations we assume a harmonic solution in the form

$$\psi(\bar{x}, \bar{t}) = D \exp(d\bar{x} + i\bar{t}), \quad (17)$$

where D and d are as yet unspecified complex constants.

Inserting the solution (17) first into the isentropic-speed equation (8), after making the transformations (15) and (16), we obtain the characteristic equation

$$d(1 + Bu_N^2) + \frac{8(\gamma_0 - 1)Bu_N}{Bo_N} + i(1 + Bu_N^2) = 0.$$

With d obtained from this equation, the solution of (8) can be written finally as

$$\psi_S(\bar{x}, \bar{t}) = D \exp\{-\delta_S \bar{x} + i(\bar{t} - \lambda_S \bar{x})\}, \quad (18)$$

where the dimensionless damping and wave speed are given respectively by

$$\delta_S = \frac{8(\gamma_0 - 1)Bu_N}{Bo_N(1 + Bu_N^2)}$$

and

$$1/\lambda_S = 1.$$

The subscript S marks these results as being the solution of the isentropic-speed equation. The solution (18) represents a right-running wave, harmonic in time, damped in distance, and travelling with precisely the isentropic speed. The region of validity (with respect to the reduced frequency $1/Bu_N$) of this and the following solutions will be discussed later.

The assumed solution (17) can similarly be used in the isothermal-speed equation (9) to obtain the solution (distinguished by subscript T)

$$\psi_T(\bar{x}, \bar{t}) = D \exp\{-\delta_T \bar{x} + i(\bar{t} - \lambda_T \bar{x})\}, \tag{19}$$

where the damping and wave speed are given by

$$\delta_T = \frac{Bo_N(\gamma_0 - 1)}{32\sqrt{\gamma_0}} \left(\frac{1}{Bu_N} + \frac{Bu_N}{\gamma_0} \right)$$

and

$$1/\lambda_T = 1/\sqrt{\gamma_0}.$$

Solution (19) represents a damped, right-running harmonic wave travelling with precisely the isothermal speed of sound.

Using the assumed solution in the infinite-speed equation (10), we obtain a quadratic characteristic equation in d , which can be solved by standard methods. The resulting solution gives

$$\psi_\infty(\bar{x}, \bar{t}) = D \exp\{-\delta_\infty \bar{x} + i(\bar{t} - \lambda_\infty \bar{x})\}, \tag{20}$$

where $\left. \begin{matrix} \delta_\infty \\ \lambda_\infty \end{matrix} \right\} = \left\{ \frac{1}{2} \left[\pm \frac{1}{1/Bu_N^2 + (16\gamma_0/Bo_N)} + \frac{Bu_N}{[1/Bu_N^2 + (16\gamma_0/Bo_N)^2]^{\frac{1}{2}}} \right] \right\}^{\frac{1}{2}}.$

The upper and lower signs go with δ_∞ and λ_∞ , respectively. In this case we have a right-running harmonic wave whose damping and wave speed both vary from zero to infinity as a function of Bu_N for any finite Bo_N . Since an infinite wave speed was followed in the derivation of (10), we expect this solution to be valid only for large wave speeds, even though very slow speeds are formally admitted.

The similarity between (10) and (11) allows us to write down the solution to the zero-speed equation (11) by analogy as

$$\psi_0(\bar{x}, \bar{t}) = D \exp\{-\delta_0 \bar{x} + i(\bar{t} - \lambda_0 \bar{x})\}, \tag{21}$$

where $\left. \begin{matrix} \delta_0 \\ \lambda_0 \end{matrix} \right\} = \left\{ \frac{1}{2} \left[\pm \frac{1}{1/Bu_N^2 + (16/Bo_N)^2} + \frac{Bu_N}{[1/Bu_N^2 + (16/Bo_N)^2]^{\frac{1}{2}}} \right] \right\}^{\frac{1}{2}}.$

This is a right-running wave with damping and wave speed also varying from zero to infinity, although these results would be expected to be valid only for small speeds.

The foregoing approximate solutions, like the differential equations from which they come, must be taken two at a time to obtain the complete solution of a

given problem. As explained in detail below, they thus provide a solution of the form,

$$\psi = D_1 \exp(d_1 \bar{x} + i\bar{t}) + D_2 \exp(d_2 \bar{x} + i\bar{t}), \quad (22)$$

for the right-running waves.

Equation (22) is also the form of the harmonic solution of the exact equation (7). Exact values for the complex constants $d_{1,2}$ can be found from the fourth-order characteristic equation,

$$d^4 \left(1 - i \frac{16Bu_N}{Bo_N}\right) + d^2 \left(1 - Bu_N^2 - i \frac{16\gamma_0 Bu_N}{Bo_N}\right) - Bu_N^2 = 0,$$

which is obtained by inserting the general harmonic solution (17) into (7). The solution of this equation for the two complex roots that represent the right-running modified-classical wave ()₁ and radiation-induced wave ()₂ (see next paragraph) is

$$d_{1,2} = - \left\{ \frac{-\left(1 - Bu_N^2 - i16\gamma_0 Bu_N/Bo_N\right) \pm \left[\left(1 - Bu_N^2 - i16\gamma_0 Bu_N/Bo_N\right)^2 + 4Bu_N^2 \left(1 - i \frac{16Bu_N}{Bo_N}\right)\right]^{\frac{1}{2}}}{2 \left(1 - i \frac{16Bu_N}{Bo_N}\right)} \right\}^{\frac{1}{2}}, \quad (23)$$

where the upper and lower signs go with 1 and 2 respectively. The complexity of this equation makes it clear why approximate methods are desirable.

To understand precisely how the four approximate solutions (18)–(21) are equivalent to the exact solution (22) and (23), we draw on the nomenclature and results introduced by Vincenti & Baldwin (1962). This is done for convenience and is in no way essential for interpreting the approximate solutions. Vincenti & Baldwin studied the two harmonic waves in the exact solution by expanding the result (23) in powers of $(\gamma_0 - 1)$. One wave was found to exhibit a small amount of damping and to travel at a speed somewhere between the only slightly different isothermal and isentropic speeds of sound. It was therefore called the ‘modified-classical wave’. The other wave travelled with both speed and damping somewhere between zero and infinity. Since this wave has no counterpart in classical acoustics, it was called the ‘radiation-induced wave’. As strongly suggested by these results, we adopt the hypothesis that our two solutions ψ_S and ψ_T correspond to the modified-classical wave, while the solutions ψ_∞ and ψ_0 correspond to the radiation-induced wave. As the analysis proceeds we shall see that this is indeed the case.

Results similar to the present approximation for the modified-classical wave (solutions (18) and (19)) have been reported by Khosla & Murgai (1965). Their results were obtained by expansions of the exact characteristic solution (23) for small and large values of the parameter $16Bu_N/Bo_N(1 + Bu_N^2)$ (their notation has been changed to coincide with that of the present analysis). Khosla & Murgai’s expression for δ_S is identical to that obtained here; their expression for δ_T is more restrictive. They do not compare their approximation with exact results, and their expansions do not produce the presently obtained results for the radiation-induced wave (solutions (20) and (21)).

By taking appropriate limits with regard to Bo_N and Bu_N in the approximate solutions and eliminating the solutions that give physically unrealistic results, one can find the ranges of these parameters in which the various approximate solutions are valid (cf. Cogley 1968, ch. 5). We can also obtain this information by comparing the approximate solutions with exact numerical results, which gives at the same time a measure of the accuracy of the approximate method. Here we use a combination of these two approaches.

Figure 1 is a plot of the damping and speed of the modified-classical wave for the small value of $Bo_N = 2 \times 10^{-3}$ (strong radiation). The exact results (obtained

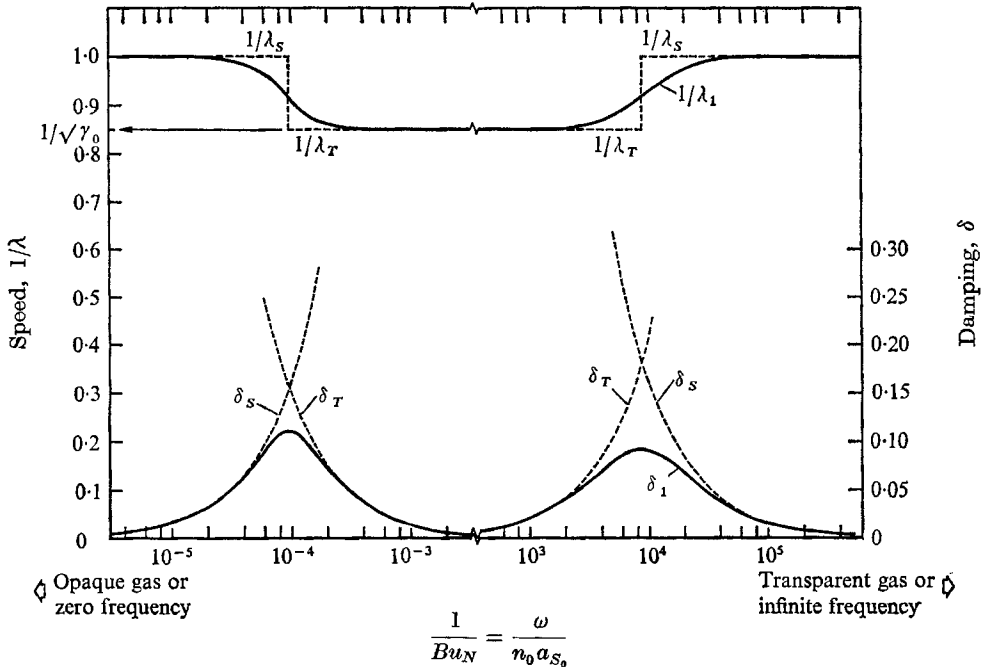


FIGURE 1. Comparison of results for damping and speed of modified-classical wave, $\gamma_0 = 1.4$, $Bo_N = 2 \times 10^{-3}$ (strong radiation). —, exact; ---, approximate. (Bo_N is defined in §3.)

from the numerical program of Long & Vincenti (1967), modified for a non-grey gas) are given as solid lines and the approximate results are dashed lines. The figure has a broken abscissa, and the exact and approximate results agree to five significant figures in the region omitted.

We see that the approximate solution for the damping is made up of the two expressions for δ_s and δ_T , which are simple second-order polynomials in $1/Bu_N$. For a thick gas or small frequencies, the isentropic-speed part of the approximate solution is valid. The analytical reason for discarding the isothermal solution here is that $\delta_T \rightarrow \infty$ as $1/Bu_N \rightarrow 0$ for finite Bo_N ; i.e. given the choice between a zero (isothermal) and finite (isentropic) contribution to the modified-classical wave, we have of course justification for choosing the latter. As $1/Bu_N$ increases, the isentropic-speed result increases and eventually intersects the isothermal-

speed result to form a peak in the damping curve. At this intersection the isothermal part of the solution becomes valid and becomes more accurate as $1/Bu_N$ increases. The transition from the isentropic to the isothermal solution can also be predicted analytically. If we stay at the Bouguer number of the intersection and let $Bo_N \rightarrow 0$, we find that $\delta_S \rightarrow \infty$ and $\delta_T \rightarrow 0$; since infinitely damped waves are negligible compared to those with zero damping, the isothermal solution must become valid at the intersection. The isothermal solution remains valid until we get to large values of $1/Bu_N$. Here the damping increases once more, with the result that the isothermal damping curve again intersects the isentropic curve. The isentropic solution thus takes over once again for very large $1/Bu_N$, and we ultimately obtain zero damping as $1/Bu_N \rightarrow \infty$. This second transition can be predicted analytically by arguments similar to those used for the first.

Equating δ_S and δ_T to find the points of intersection leads to a fourth-order polynomial in $1/Bu_N$. For small Bo_N this polynomial has the approximate positive roots,

$$1/Bu_N \cong Bo_N/16\gamma_0^{\frac{1}{2}} \quad (24a)$$

and
$$1/Bu_N \cong 16\gamma_0^{\frac{1}{2}}/Bo_N. \quad (24b)$$

These roots agree closely with the values of $1/Bu_N$ for which the exact solution for δ has its maxima. At these intersection points, the approximate value of the wave speed is shown in the figure as changing discontinuously from the isentropic to the isothermal value, since the wave speed must correspond to the appropriate damping curve. The exact value of the wave speed goes through a rapid variation near the transition points as shown.

Although not apparent from figure 1, δ_S is a continuous curve with a maximum and δ_T a continuous curve with a minimum. As the non-grey Boltzmann number increases, the curves (and their respective maximum and minimum) move toward each other linearly with Bo_N and become tangent for Bo_N of order $16\sqrt{\gamma_0}$. For the slightly larger Bo_N of 20, we obtain the results shown in figure 2. We now discard completely the isothermal part of the approximate solution, since an intersection never takes place. The exact solution, however, still shows evidence of a slight change in wave speed for values of $1/Bu_N$ around unity. As Bo_N becomes still larger, the exact and isentropic approximate solutions for the modified-classical wave become indistinguishable for all $1/Bu_N$.

In general, the approximate solution for the modified-classical wave gives accurate results everywhere except over small regions of $1/Bu_N$ in which transitions from the isentropic to the isothermal solution take place when $Bo_N \ll 16\sqrt{\gamma_0}$. For $Bo_N \gg 16\sqrt{\gamma_0}$, only the isentropic part of the approximate solution is valid, and its accuracy is good for all $1/Bu_N$.

Figure 3 presents the damping and wave speed for the radiation-induced wave at the previous low value of $Bo_N = 2 \times 10^{-3}$ (strong radiation). For this wave the approximate solutions do not intersect, but the transition from the zero- to the infinite-speed results takes place at values of $1/\lambda_2$ of about 2 as indicated by the exact solution. This occurs in the range of values of $1/Bu_N$ at which the left-hand peak appeared for the damping of the modified-classical wave in figure 1, i.e. for values of $1/Bu_N$ given by (24a). The transition region follows this value of

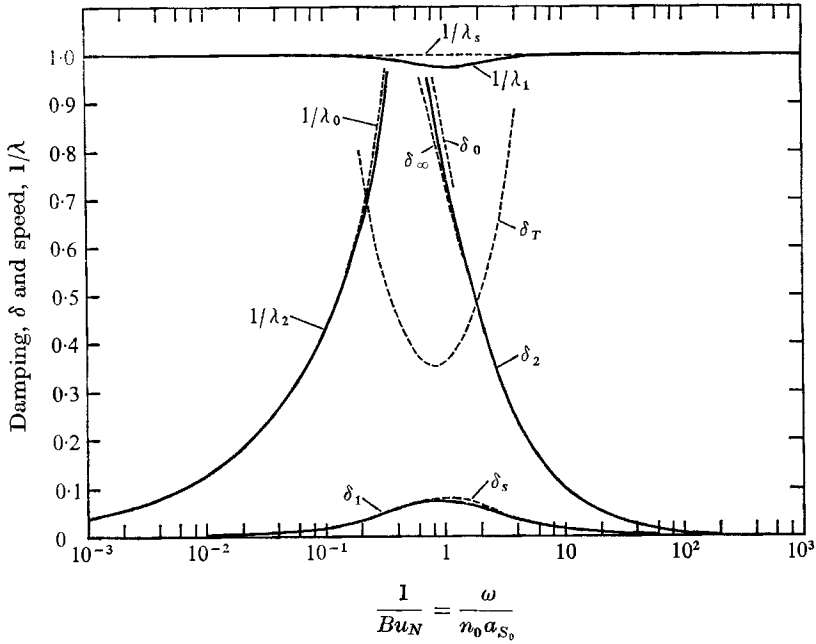


FIGURE 2. Comparison of results for damping and speed of both waves, $\gamma_0 = 1.4$, $Bu_N = 20$. —, exact; --- approximate.

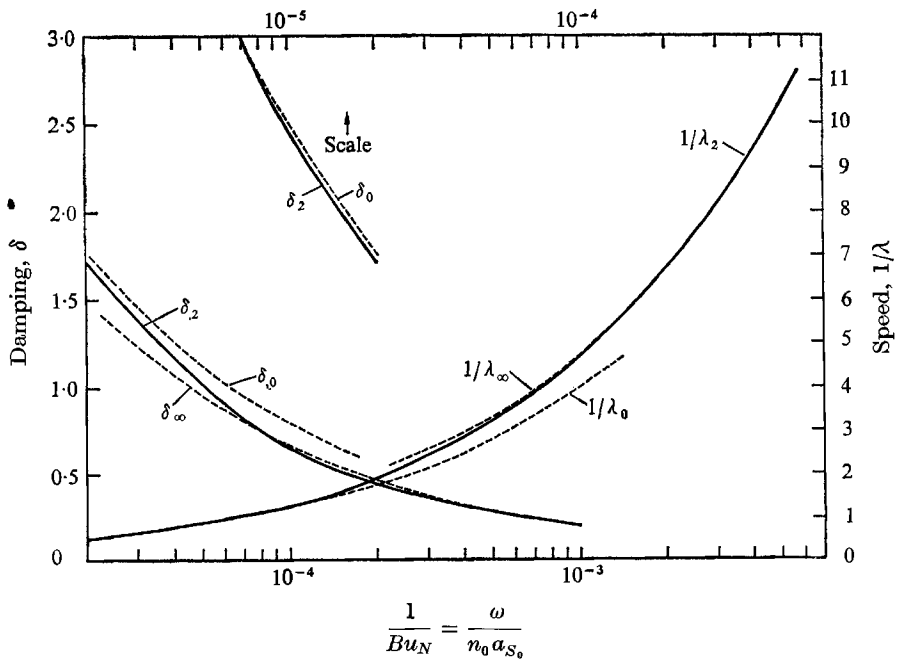


FIGURE 3. Comparison of results for damping and speed of radiation-induced wave, $\gamma_0 = 1.4$, $Bu_N = 2 \times 10^{-3}$ (strong radiation). —, exact; ---, approximate.

$1/Bu_N$ for all $Bo_N \ll 16\sqrt{\gamma_0}$. Comparison with the exact solution, however, is a cumbersome means for fixing the transition region for the radiation-induced wave. Consistent with our mathematical assumptions, the analytical criterion to be used is that the infinite-speed solution is valid when $1/\lambda \gg 1$, and the zero-speed solution when $1/\lambda \ll 1$.

A typical result for the radiation-induced wave for $Bo_N > 16\sqrt{\gamma_0}$ has already been included in figure 2. The complete transition is not visible in this figure, but it is clear that it now takes place near $1/Bu_N = 1$. This location for the transition region holds for all larger values of Bo_N .

The question of which approximate solution or equation is valid for specific ranges of reduced frequency $1/Bu_N$ has thus been answered. For convenience, the results are summarized in table 1.

Type of wave	Approximate solution	Region of validity	
		$Bo_N \gg 16\sqrt{\gamma_0}$	$Bo_N \ll 16\sqrt{\gamma_0}$
Modified-classical	Isentropic-speed solution (18)	All $1/Bu_N$	$\begin{cases} 1/Bu_N > 16/Bo_N \\ 1/Bu_N < Bo_N/16\gamma_0 \end{cases}$
	Isothermal-speed solution (19)	Not valid	$Bo_N/16\gamma_0 < 1/Bu_N < 16/Bo_N$
Radiation-induced	Infinite-speed solution (20)	$1/Bu_N > 1$	$1/Bu_N > Bo_N/16\gamma_0$
	Zero-speed solution (21)	$1/Bu_N < 1$	$1/Bu_N < Bo_N/16\gamma_0$

TABLE 1

Here we have set $\gamma_0^{\frac{1}{2}} \cong \gamma_0$ and $\gamma_0^{\frac{1}{2}} \cong 1$ in (24a) and (24b), respectively, to simplify matters. We are at liberty to do this because γ_0 is of order unity and the transition regions are not sharply defined anyway.

We now proceed to the magnitude of the harmonic waves. The dependence of the harmonic solution on the boundary conditions is best seen by studying the response of the gas to the motion of a constant-temperature wall and to the temperature variation of a motionless wall. These two driving disturbances can be conveniently written as

$$u_w = \frac{A}{\gamma_0} e^{it} \quad (\text{velocity})$$

and
$$\frac{dT_w(\bar{t})}{d\bar{t}} = B e^{it} \quad (\text{temperature}),$$

where the dimensionless constants A and B are real, and γ_0 is introduced for consistency with the existing literature. The corresponding boundary conditions on ψ are found by putting these expressions into (12) and (13) and making the necessary change of variables given by equations (15) and (16). Substituting the solution (22) into the resulting relations and carrying out certain simplifications, one then obtains two equations for D_1 and D_2 , which can be solved simultaneously to find the wave magnitudes (absolute value of the amplitudes) for the two special cases of (i) A given, $B = 0$ and (ii) B given, $A = 0$. The results give expressions for $|D_1/A|_{B=0}$, $|D_2/A|_{B=0}$ and $|D_1/B|_{A=0}$, $|D_2/B|_{A=0}$, as functions of γ_0 , Bu_N , d_1 and d_2 . To this point the procedure is exact. Approximate results for the

amplitudes are then found by substituting the approximate values for d_1 and d_2 in accord with the previous findings; i.e. for the modified-classical wave

$$d_1 = -(\delta_S + i\lambda_S) \quad \text{or} \quad d_1 = -(\delta_T + i\lambda_T),$$

and for the radiation-induced wave

$$d_2 = -(\delta_\infty + i\lambda_\infty) \quad \text{or} \quad d_2 = -(\delta_0 + i\lambda_0).$$

Which alternative is used in each case depends on the regions of validity as given in the table. Since the δ 's and λ 's are functions of γ_0 , Bu_N and Bo_N , we finally obtain the approximate results for the wave magnitudes as functions of these three parameters (cf. Cogley 1968, ch. 5).

Vincenti & Baldwin also developed approximate expressions for the wave magnitudes by expansions in powers of $(\gamma_0 - 1)$ and presented qualitative plots. The exact wave magnitudes can be found by using the results for d_1 and d_2 obtained from (23) by means of the numerical program of Long & Vincenti.

A comparison between the present approximation and the exact results is given by Cogley (1968). The results show that the approximation for the wave magnitudes is as accurate as that for the damping and wave speed. This is to be expected, since the wave magnitudes are known as exact functions of these quantities. Moreover, it is found that the present results provide more accurate details than do Vincenti & Baldwin's results obtained by power expansions.

The harmonic solution demonstrates that the approximate method is capable of providing accurate quantitative results. The knowledge gained about the lower-order equations and their regions of validity is also necessary for application in the more difficult study of discrete waves.

5. Discrete waves

In this section we set down the formalism for the problem of a discrete wave caused by simultaneous step inputs of wall velocity and temperature. We shall later use this formalism to obtain the detailed solution for an impulsively started constant-temperature wall in §6 and for a discontinuously heated stationary wall in Cogley (1969).

For background we first examine the exact problem. The exact governing equation is (6). The boundary conditions (which apply later also to the approximate solution) are (12)–(24), where the driving disturbances are now

$$u_w(\tau) = \begin{cases} 0 & (\tau < 0), \\ u_w(\text{constant}) & (\tau > 0), \end{cases} \tag{25}$$

and
$$T_w(\tau) = \begin{cases} 0 & (\tau < 0), \\ T_w(\text{constant}) & (\tau > 0). \end{cases} \tag{26}$$

The initial conditions are homogeneous to all orders, i.e. the gas is initially quiescent.

We proceed formally by taking the Laplace transform of (6). The result is

$$M\bar{\phi}_{\xi\xi\xi\xi} - N\bar{\phi}_{\xi\xi} + s^3\bar{\phi} = 0, \tag{27}$$

where
$$\bar{\phi}(\xi, s) \equiv \int_0^\infty \phi(\xi, \tau) e^{-s\tau} d\tau,$$

and we have introduced the definitions

$$M \equiv s + 16/Bo_N, \quad N \equiv s(s^2 + 16\gamma_0 s/Bo_N + 1).$$

The bar denotes a transformed quantity, and s is the independent variable in transform space. Subject to the far boundary conditions, the solution of (27) (as well as the approximate transformed solution, see below) can be written as

$$\phi(\xi, s) = C_I \exp(c_I \xi) + C_{II} \exp(c_{II} \xi), \tag{28}$$

where for the exact solution we have

$$c_{I,II} = - \left[\frac{N}{2M} \pm \frac{1}{2M} (N^2 - 4s^3 M)^{\frac{1}{2}} \right]^{\frac{1}{2}}. \tag{29}$$

The subscripts I and II in (28) are deliberately different from the 1 and 2 in the harmonic solution of §4 for reasons that will appear presently.

The constants C_I and C_{II} are found by taking the Laplace transform of the boundary conditions (12) and (13) specialized to the disturbances (25) and (26). Substituting solution (28) into the transformed results and carrying out certain simplifications, we obtain a pair of simultaneous equations, whose solution can be written as

$$C_I = \frac{u_w}{s c_I} - C_{II} \frac{c_{II}}{c_I}, \tag{30}$$

and
$$C_{II} = \frac{(u_w/s)(\gamma_0 s^2 - c_I^2)(c_{II} + 1) + T_w c_I (c_I + 1)(c_{II} + 1)}{c_{II}(\gamma_0 s^2 - c_I^2)(c_{II} + 1) - c_I(\gamma_0 s^2 - c_{II}^2)(c_I + 1)}. \tag{31}$$

The formal solution of the exact governing equation can be written in terms of the inversion formula as

$$\phi(\xi, \tau) = \frac{1}{2\pi i} \int_{\Gamma} \{C_I \exp(s\tau + c_I \xi) + C_{II} \exp(s\tau + c_{II} \xi)\} ds, \tag{32}$$

where Γ signifies an appropriate Bromwich path of integration. The integral represents the superposition of harmonic waves, with s corresponding to the frequency. One cannot, however, identify term I exclusively with the modified-classical waves nor term II with the radiation-induced waves (hence the difference in notation from §4). We are therefore not readily able to use the exact results for harmonic waves to obtain the exact solution for the discrete wave. As we shall explain, on the other hand, the approximate method does allow us to identify the terms in the foregoing way and hence to use the results of §4 in our approximate treatment.

Since c_I , c_{II} , C_I and C_{II} are such complicated functions of s , a complete investigation of the exact solution (32) is not feasible, except possibly by numerical means. Instead, we shall study the problem here on the basis of the approximate governing equations developed in §3. These lower-order equations can be Laplace transformed and solved easily in the transformed variable. The results and their regions of validity are as listed below.

Equation (8):

$$\left. \begin{aligned} \bar{\phi}_S(\xi, s) &= C \exp(c_S \xi), \quad c_S = -s - \frac{8(\gamma_0 - 1) s^2}{Bo_N(s^2 - 1)}, \\ Bo_N \gg 16\sqrt{\gamma_0}: \text{ all } |s|; \quad Bo_N \ll 16\sqrt{\gamma_0}: |s| < Bo_N/16\gamma_0, |s| > 16/Bo_N. \end{aligned} \right\} \tag{33}$$

Equation (9):

$$\left. \begin{aligned} \bar{\phi}_T(\xi, s) = C \exp(c_T \xi), \quad c_T = -s\sqrt{\gamma_0} + \frac{Bo_N(\gamma_0 - 1)s^2}{32\sqrt{\gamma_0}} - \frac{Bo_N(\gamma_0 - 1)}{32\gamma_0^{\frac{3}{2}}}, \\ Bo_N \gg 16\sqrt{\gamma_0}: \text{ not valid; } \quad Bo_N \ll 16\sqrt{\gamma_0}: Bo_N/16\gamma_0 < |s| < 16/Bo_N. \end{aligned} \right\} \quad (34)$$

Equation (10):

$$\left. \begin{aligned} \bar{\phi}_\infty(\xi, s) = C \exp(c_\infty \xi), \quad c_\infty = -\left(\frac{s}{s + 16\gamma_0/Bo_N}\right)^{\frac{1}{2}}, \\ Bo_N \gg 16\sqrt{\gamma_0}: |s| > 1; \quad Bo_N \ll 16\sqrt{\gamma_0}: |s| > Bo_N/16\gamma_0. \end{aligned} \right\} \quad (35)$$

Equation (11):

$$\left. \begin{aligned} \bar{\phi}_0(\xi, s) = C \exp(c_0 \xi), \quad c_0 = -\left(\frac{s}{s + 16/Bo_N}\right)^{\frac{1}{2}}, \\ Bo_N \gg 16\sqrt{\gamma_0}: |s| < 1; \quad Bo_N \ll 16\sqrt{\gamma_0}: |s| < Bo_N/16\gamma_0. \end{aligned} \right\} \quad (36)$$

Since $|s|$ corresponds directly to $1/Bu_N$ (a reduced frequency), the regions of validity given after each solution are obtained from the results for harmonic waves in table 1. When these solutions are inverted, the first two represent a superposition of the modified-classical harmonic waves, and the second two represent a superposition of the radiation-induced waves.

The complete approximate solution is the sum of two of the above solutions, one from the modified-classical pair and one from the radiation-induced pair. Which one is to be used for each pair for a given value of s depends on the region of Bo_N that is of interest. The approximate transformed solution thus has the same form as (28), but with the appropriate quantities c_S , c_T , c_∞ or c_0 inserted. Specifically, we let c_I be either c_S or c_T , which means that the first term in (28) is now associated purely with the modified-classical waves. The quantity c_{II} is then replaced by either c_∞ or c_0 , so that the second term represents the radiation-induced waves. The notation C_I and C_{II} will be retained, and we thus henceforth associate these quantities in our approximate solutions with the modified-classical and radiation-induced contributions, respectively. Hence, we write the transform of the approximate solution as

$$\bar{\phi}(\xi, s) = C_I \exp\{(\text{either } c_S \text{ or } c_T)\xi\} + C_{II} \exp\{(\text{either } c_\infty \text{ or } c_0)\xi\}, \quad (37)$$

where we note from (30) and (31) that C_I and C_{II} are functions of c_S or c_T , and c_∞ or c_0 , as well as u_w , T_w , γ_0 and s .

Even (37) cannot easily be inverted, and indeed we do not want to invert it as it stands. When Bo_N is small, for example, c_S applies only for $|s| < Bo_N/16\gamma_0$ and $|s| > 16/Bo_N$. It follows that it is then unnecessary to attempt an inversion of (37) for all s . Instead, we need only make appropriate expansions for large and small s and use the Abelian initial- and final-value theorems for the Laplace transformation to interpret the results. These theorems relate the asymptotic behaviour of a function $f(t)$ as $t \rightarrow 0_+$ or ∞ to the asymptotic behaviour of $\bar{f}(s)$ as $s \rightarrow \infty$ or 0_+ , respectively.

The solutions obtained by this method are general in the sense that they cover the entire range of Boltzmann number and are valid for all values of the absorp-

tion coefficient. They are approximate in that they are restricted to specified small-, intermediate- and large-time regions. These regions correspond to the frequency regions (or more precisely to the regions of $1/Bu_N$) in which the approximate harmonic solutions were shown to be valid (cf. table 1). The transition from one time region to the next is fairly rapid, just as the transitions in frequency space were rapid. The evolution of the wave-form is therefore easily followed, and the approximate method does not lose any information essential for obtaining the correct physical view of the overall wave phenomena.

Since the potential function is not in itself of interest, we will invert only the physical quantities, i.e. the perturbation pressure, velocity, density and temperature. These quantities are most directly found by use of the properties of the Laplace transformation. The pressure, for example, is related to ϕ by $p = -\gamma_0 \partial\phi/\partial\tau$, and the transform of this equation is

$$\bar{p} = -\gamma_0 \{s\bar{\phi} - \phi(\xi, 0)\}. \quad (38)$$

Since $\phi(\xi, 0)$ can be taken as zero, this provides a simple relation between \bar{p} and $\bar{\phi}$. The transforms of the other physical quantities, found by similar arguments, are given by

$$\bar{u} = \partial\bar{\phi}/\partial\xi, \quad (39)$$

$$\bar{\rho} = -(1/s) \partial^2\bar{\phi}/\partial\xi^2, \quad (40)$$

and

$$\bar{T} = \bar{p} - \bar{\rho}. \quad (41)$$

For a mechanically driven discrete wave ($u_w \neq 0, T_w = 0$), Whitham's qualitative results can be used to predict the form of the solution without solving the lower-order equations. The same cannot be done for the radiatively driven discrete wave ($u_w = 0, T_w \neq 0$), since it has a fundamentally different driving mechanism not considered by Whitham. We therefore do not utilize this part of Whitham's work or attempt a generalization, but proceed directly to our detailed solutions.

6. Mechanically driven discrete wave

Our reconsideration of the mechanically driven discrete wave was conceived originally as merely a learning exercise in the application of the approximate method. The analysis revealed, however, certain results not obtained by previous investigators using other approximate methods.

The phenomenology that will develop from the solution is summarized schematically in figure 4. This figure is presented now to provide a frame of reference as the solution proceeds. It is an order-of-magnitude plot in Bo_N, τ plane; it shows where the various parts of the approximate solution are valid and where certain physical phenomena take place. The detailed solution will be exhibited for the case of $Bo_N \gg 16\sqrt{\gamma_0}$ (weak radiation); for $Bo_N \ll 16\sqrt{\gamma_0}$ (strong radiation) only a general discussion will be given. Such discussion is possible with the help of figure 4, since the phenomenology of the two cases is similar. The reader interested in more detail will find it in Cogley (1968).

To obtain the solution for $Bo_N \gg 16\sqrt{\gamma_0}$ and small time, we appeal to the Abelian theorems and expand the appropriate c 's and the C 's (given respectively

by (33), (35) and (30), (31) with $T_w = 0$ for $|s| \gg 1$. With the definition $g \equiv 8(\gamma_0 - 1)/Bo_N$, this leads to the following results:

$$c_S = -s - g + O(g/s^2),$$

$$c_\infty = -1 + O(8\gamma_0/Bo_N s),$$

$$C_I = \frac{u_w}{s(-s-g)} + O(u_w g/s^5),$$

$$C_{II} = -\frac{u_w g}{s^4} + O(u_w g/s^5). \dagger$$

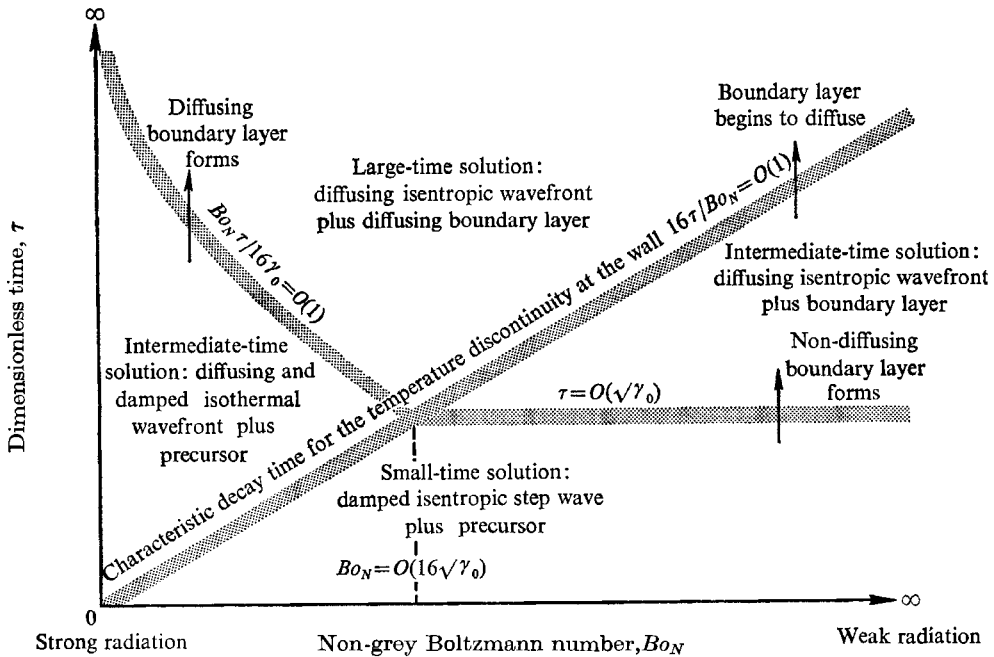


FIGURE 4. Schematic representation of solution for the mechanically driven plane wave. \square , transition regions.

These truncated expressions can now be used in conjunction with the solution (37) and (38)–(41) to obtain the transformed dependent variables. The inversions are readily carried out by means of tables (cf. Erdelyi *et al.* 1954), and the results to $O(\tau^2)$ are

$$\frac{u}{u_w} \approx e^{-g\xi} S(\tau - \xi), \tag{42}$$

$$\frac{p}{u_w} \approx \gamma_0 e^{-g\tau} S(\tau - \xi) + \gamma_0 g \frac{\tau^2}{2} e^{-\xi}, \tag{43}$$

$$\frac{\rho}{u_w} \approx e^{-g\xi} [1 + g(\tau - \xi)] S(\tau - \xi), \tag{44}$$

$$\frac{T}{u_w} \approx \{ \gamma_0 e^{-g\tau} - e^{-g\xi} [1 + g(\tau - \xi)] \} S(\tau - \xi) + \gamma_0 g \frac{\tau^2}{2} e^{-\xi}, \tag{45}$$

† The parameter g is introduced for brevity, since it is a basic parameter of the modified-classical contribution. It is not, however, characteristic of the radiation-induced contribution, so the main over-all parameter is still the Boltzmann number Bo_N .

where the unit step function is defined by

$$S(\tau - \xi) = \begin{cases} 1 & \xi < \tau, \\ 0 & \xi > \tau. \end{cases}$$

As indicated in figure 4 this solution is valid for $\tau < \sqrt{\gamma_0}$, or equivalently for $\tau < 1$ to the precision that we are determining the time regions. The terms containing the step function are the modified-classical contribution; those with the exponential $e^{-\xi}$ are the radiation-induced effects. The major portion of the response is given by the step wave, which travels at the isentropic speed of sound (i.e. such that $\xi = \tau$) and is exponentially damped. The radiation-induced contribution is small in this time region, affecting only the pressure and temperature to the present order. It provides a precursor ahead of the step wave. The temperature of the gas at $\xi = 0$ is not equal to that of the wall (i.e. $T(0, \tau) \neq 0$), because molecular conduction has been neglected. In this time region the step wave has travelled less than one radiative mean free path, which corresponds to $\xi = 1$.

The solution for $Bo_N \gg 16\sqrt{\gamma_0}$ and intermediate time, which corresponds to small but finite values of $|s|$ through the Abelian theorems, is found by expanding the expressions for the appropriate c 's and the C 's in the annular region $16/Bo_N < |s| < 1$. The restriction that $16/Bo_N < |s|$ is dictated by the structure of c_0 , (36), which we want to expand. The expansions give

$$\begin{aligned} c_S &= -s + gs^2 + O(gs^4), \\ c_0 &= -1 + O(8/Bo_N s), \\ C_I &= \frac{u_w}{s(-s + gs^2)} + O(u_w g/s^2), \\ C_{II} &= -\frac{u_w g}{s} + O[u_w(\gamma_0 - 1)(16/Bo_N s)^2]. \end{aligned}$$

Using the procedure outlined earlier, we can obtain expressions for the transformed dependent variables. The inversion of the resulting modified-classical terms is made by the method of steepest descent. The procedure is standard, similar to that used by Lick (1964), and given in detail Cogley (1968). The radiation-induced terms are again inverted by means of tables. The results to $O(16\tau/Bo_N)$ are

$$\frac{u}{u_w} \cong \left\{ 1 - \frac{1}{2} \operatorname{erfc} \left[\frac{(\tau - \xi)}{2\sqrt{g\xi}} \right] \right\}, \tag{46}$$

$$\frac{p}{u_w} \cong \gamma_0 \left\{ 1 - \frac{1}{2} \operatorname{erfc} \left[\frac{(\tau - \xi)}{2\sqrt{g\xi}} \right] + \frac{1}{2} \left(\frac{g}{\pi\xi} \right)^{\frac{1}{2}} \exp \left[-\frac{(\tau - \xi)^2}{4g\xi} \right] \right\}, \tag{47}$$

$$\frac{\rho}{u_w} \cong \left\{ 1 - \frac{1}{2} \operatorname{erfc} \left[\frac{(\tau - \xi)}{2\sqrt{g\xi}} \right] - \frac{1}{2} \left(\frac{g}{\pi\xi} \right)^{\frac{1}{2}} \exp \left[-\frac{(\tau - \xi)^2}{4g\xi} \right] \right\} + g\tau e^{-\xi}, \tag{48}$$

and
$$T = p - \rho. \tag{49}$$

The modified-classical contribution (the terms in braces) now represent a diffusing isentropic wave (note that the third term in the braces for p, ρ and T is small). The wave is no longer damped because the radiation emitted in the region of the wave-front (i.e. near $\xi = \tau$) is re-absorbed within the wave-front, which is now

a number of radiative mean free paths thick. This, in fact, is the mechanism for the diffusion of the wave. The modified-classical contribution is now seen to provide its own precursor as a result of this diffusion. The radiation-induced contribution is now felt predominantly behind the wave-front (i.e. for $\xi \ll \tau$) and represents a non-diffusing boundary layer next to the wall. Thus, we see that the radiation-induced contribution does not have a continuous identity from the small- to the intermediate-time region.† This boundary layer affects only the density and temperature to the present order, and this effect grows linearly with time. From the temperature solutions for small and intermediate time, we see that the temperature discontinuity at the wall ($\xi = 0$) decreases, to first order, linearly with time, i.e. we pick up predominantly the linear part of the variation in our expansion. At the end of the intermediate-time region this discontinuity essentially disappears (cf. figure 4), since $g\tau$ there approaches $O(\gamma_0 - 1)$. The boundary layer, a radiation-induced effect, thus provides the mechanism for ultimately eliminating the temperature discontinuity at the wall, a result that is obviously necessary as a consequence of the radiation from the gas.

In the limit as $Bo_N \rightarrow \infty$, the small- and intermediate-time solutions make up the total solution. Taking this limit in (42)–(49), we in fact obtain identical results for the two time regions. The radiation-induced contribution goes to zero, and the modified-classical contribution goes to the classical result of an undamped isentropic step wave. This is the same result that one obtains by first taking this limit in the exact governing equation (6) and then solving the resulting simplified problem.

The large-time solution is obtained by expanding the appropriate expressions for $|s| < 16/Bo_N$ (i.e. for $|s| \rightarrow 0$). The results are

$$\begin{aligned} c_s &= -s + gs^2 + O(gs^4), \\ c_0 &= -(Bo_N s/16)^{\frac{1}{2}} + O((Bo_N s/16)^{\frac{3}{2}}), \\ C_I &= \frac{u_w}{s(-s + gs^2)} + O\left(u_w \left(\frac{16}{Bo_N}\right)^{\frac{1}{2}} \frac{(\gamma_0 - 1)}{s^{\frac{3}{2}}}\right), \\ C_{II} &= -\frac{u_w 2g}{s} + O\left(u_w(\gamma_0 - 1) \left(\frac{16}{Bo_N s}\right)^{\frac{1}{2}}\right). \end{aligned}$$

The inversions for the modified-classical terms in the resulting transformed variables have already been carried out in the intermediate-time solution; those for the radiation-induced terms can again be found from tables. The solution, when terms of $O((Bo_N/16\tau)^{\frac{1}{2}})$ are dropped, is

$$\frac{u}{u_w} \cong \left\{ 1 - \frac{1}{2} \operatorname{erfc} \left[\frac{(\tau - \xi)}{2\sqrt{g\xi}} \right] \right\}, \tag{50}$$

$$\frac{p}{u_w} \cong \gamma_0 \left\{ 1 - \frac{1}{2} \operatorname{erfc} \left[\frac{(\tau - \xi)}{2\sqrt{g\xi}} \right] + \frac{1}{2} \left(\frac{g}{\pi\xi} \right)^{\frac{1}{2}} \exp \left[-\frac{(\tau - \xi)^2}{4g\xi} \right] \right\}, \tag{51}$$

$$\frac{\rho}{u_w} \cong \left\{ 1 - \frac{1}{2} \operatorname{erfc} \left[\frac{(\tau - \xi)}{2\sqrt{g\xi}} \right] - \frac{1}{2} \left(\frac{g}{\pi\xi} \right)^{\frac{1}{2}} \exp \left[-\frac{(\tau - \xi)^2}{4g\xi} \right] \right\} + (\gamma_0 - 1) \operatorname{erfc} \left[\frac{\xi}{2} \left(\frac{Bo_N}{16\tau} \right)^{\frac{1}{2}} \right], \tag{52}$$

and
$$T = p - \rho. \tag{53}$$

† The reasons behind this at first disconcerting result are discussed in connexion with figure 6 of Cogley (1969).

The diffusing wave front given by the modified-classical contribution (in braces) is mathematically identical to that observed at intermediate time. Physically, however, because of the larger values of τ and ξ , the wave front is now many radiative mean free paths thick, and the precursor formed by diffusion is more pronounced. The radiation-induced contribution, on the other hand, has undergone an essential change between the intermediate- and large-time regions.† The boundary layer next to the wall now has an effect of constant magnitude on the density and temperature at $\xi = 0$, and a region of influence that grows as $\sqrt{\tau}$. It has therefore become a diffusing boundary layer. As time increases, the boundary layer becomes thin with respect to the total width of the compressively heated gas, which grows as τ . The ratio of the widths of the wave-front and boundary layer are independent of time in this region. Characteristic measures of these two widths are found by setting $|\tau - \xi|/2\sqrt{g\xi} \cong |\tau - \xi|/2\sqrt{g\tau} = 1$ and $(\xi/2)(Bo_N/16\tau)^{\frac{1}{2}} = 1$, respectively, and their ratio at a given time is

$$\frac{\text{wave-front width}}{\text{boundary-layer width}} = \frac{|\tau - \xi|}{\xi} = \left[\frac{(\gamma_0 - 1)}{2} \right]^{\frac{1}{2}}. \quad (54)$$

Thus the widths of the two phenomena of interest are of the same order. Moreover, the wave-front and boundary layer cause equally large perturbations in the temperature. The boundary layer can therefore never be assumed negligible, even for weak radiation.

The complete picture of the response for $Bo_N \gg 16\sqrt{\gamma_0}$ can now be summarized (cf. figure 4). At small time the modified-classical contribution is an exponentially decaying step wave at $\xi = \tau$; the radiation-induced contribution forms a small precursor ahead of this wave. For intermediate times, the modified-classical contribution gives a diffusing isentropic-speed wave centred about $\xi = \tau$. This contribution contains its own precursor by virtue of the diffusion. The radiation-induced contribution now produces a non-diffusing boundary layer next to the wall which increases the density and decreases the temperature, relative to the values produced by the passage of the isentropic-speed wave. The velocity and pressure, however, are unaffected to the present order. The effect of this boundary layer grows with time, so that the temperature discontinuity at the wall is effectively eliminated by the end of this region. At large times, the isentropic-speed wave continues to diffuse around $\xi = \tau$, but the boundary-layer effect now has a constant magnitude at $\xi = 0$ and increases in width as $\sqrt{\tau}$. Its physical effect, however, is a continuation of that observed at intermediate time.

The results for $Bo_N \ll 16\sqrt{\gamma_0}$ (strong radiation) will now be described without going through the details. At small time (cf. figure 4), the modified-classical contribution again gives a damped isentropic-speed step wave at $\xi = \tau$, and the radiation-induced contribution again produces a small precursor ahead of this wave. The only difference from the situation for $Bo_N \gg 16\sqrt{\gamma_0}$ is that the wave is now more highly damped and the precursor is more pronounced owing to the increased radiative transfer. For the same reason, the temperature discontinuity

† The contribution does, however, have continuous physical identity from the intermediate- to the large-time region.

at the wall is now essentially eliminated by the end of this time region. For intermediate times, the modified-classical contribution gives a damped and diffusing isothermal-speed wave centred around $\xi = \tau/\sqrt{\gamma_0}$. This wave-front has a characteristic width of less than one radiative mean free path throughout most of the time region. Much of the radiant energy from the compressed gas escapes through the wave front, causing it to decay, and shows up as a precursor that is given mathematically by the radiation-induced contribution. A certain amount of radiation is also absorbed in the wave front, suppressing any temperature variation and causing diffusion. At large times the structure of the solution changes. The modified-classical contribution (a diffusing wave front) returns to being centred on the isentropic characteristic ($\xi = \tau$). This comes about because it is now many radiative mean free paths thick, with the result that heat transfer is negligible within the wave front. This contribution produces its own precursor through diffusion. The radiation-induced contribution is now felt predominantly behind the isentropic wave front, where it provides a diffusing boundary layer next to the wall. Within this boundary layer the temperature decreases and the density increases relative to the values behind the isentropic wave; the pressure and velocity are unaffected to the order of the solution. The solution at large time is thus similar to that for $Bo_N \gg 16\sqrt{\gamma_0}$, except that the wave front and boundary layer are now much thicker owing to the higher level of radiative transfer. Again, as in the case of weak radiation, the approximate method has allowed us to handle the radiation-induced contribution (the boundary layer and a part of the precursor).

Finally, the relation between this and previous work must be mentioned. Baldwin (1962) and Lick (1964), using expansions of a solution of the complete potential equation, obtained results only for the velocity response. Although Lick's potential solution included only the modified-classical contribution, his results can be shown to compare well with the more complete treatments of Baldwin and ourselves. This is because, as we have seen, the radiation-induced contribution has only a second-order effect on the velocity. Baldwin further discussed the temperature correctly in a qualitative way, including the presence of the boundary layer near the wall. This layer was also discussed briefly by Lick (1967) in a survey article; it would have been missing from his earlier analysis because of the absence of the radiation-induced contribution. Moore (1966), using the approximation that γ_0 is close to unity, solved for the temperature as well as the velocity. His basic approximation has the effect of dropping the radiation-induced contribution, which must then be recovered by a different expansion procedure. Moore did this for the case of strong radiation, giving an account of the development of the velocity and temperature profiles that is physically equivalent to that outlined above for $Bo_N \ll 16\sqrt{\gamma_0}$. By treating the modified-classical and radiation-induced contributions simultaneously and consistently throughout, the present method is able to obtain results, uniformly valid in space, for the development of the flow field for all regions of Bo_N and τ . In particular, it gives the details of the thermal boundary layer that exists even for weak radiation and that is essential for the final elimination of the temperature jump at the wall.

With the success of the approximate method demonstrated, we are now in a position to use it in solving new problems. One such problem is treated in Cogley (1969) (the following, companion paper).

The authors thank Prof. G. B. Whitham of the California Institute of Technology for a helpful discussion of the basic approximation. The work was supported by the U.S. Air Force Office of Scientific Research, contract AF 49(638)-1280. During part of the study A. C. Cogley received a National Aeronautics and Space Administration Training Grant.

REFERENCES

- BALDWIN, B. S. 1962 The propagation of plane acoustic waves in a radiating gas. *NASA TR R-138*.
- CHENG, P. 1966 Dynamics of a radiating gas with application to flow over a wavy wall. *AIAA J.* **4**, 238.
- COGLEY, A. C. 1968 An approximate method of analyzing non-equilibrium acoustic phenomena with application to discrete radiation-driven waves. Ph.D. Thesis, Dept. of Aero. and Astro., Stanford University.
- COGLEY, A. C. 1969 The radiatively driven discrete acoustic wave. *J. Fluid Mech.* **39**, 667.
- COURANT, R. & HILBERT, D. 1962 *Methods of Mathematical Physics*. vol. II. New York: Interscience.
- ERDELYI, A. *et al.* 1954 *Tables of Integral Transforms*. New York: McGraw Hill.
- GILLES, S. E., COGLEY, A. C. & VINCENTI, W. G. 1969 A substitute-kernel approximation for radiative transfer in a non-grey gas near equilibrium, with application to radiative acoustics. *Int. J. Heat and Mass Transfer*, **12**, 445.
- KHOSLA, P. K. & MURGAI, M. P. 1965 Small amplitude wave propagation in hot ionized gases. *Phys. Fluids*, **8**, 2087.
- LICK, W. J. 1964 The propagation of small disturbances in a radiating gas. *J. Fluid Mech.* **18**, 274.
- LICK, W. J. 1967 Wave propagation in real gases. *Advan. Appl. Mech.* **10**, Fasc. 1.
- LONG, H. R. & VINCENTI, W. G. 1967 Radiation-driven acoustic waves in a confined gas. *Phys. Fluids*, **10**, 1365.
- MOORE, F. K. 1966 Effect of radiative transfer on a sound wave travelling in a gas having γ near one. *Phys. Fluids*, **9**, 70.
- VINCENTI, W. G. & BALDWIN, B. S. 1962 Effect of thermal radiation on the propagation of plane acoustic waves. *J. Fluid Mech.* **12**, 449.
- VINCENTI, W. G. & KRUGER, C. H. 1965 *Introduction to Physical Gas Dynamics*. New York: Wiley.
- WHITHAM, G. B. 1959 Some comments on wave propagation and shock wave structure with application to magnetohydrodynamics. *Comm. Pure Appl. Math.* **12**, 113.